

A new on-line state-of-health monitoring technique dedicated to PEM fuel cell

O. Bethoux, *Member IEEE*, M. Hilairret, *Member IEEE*, and T. Azib
Laboratoire de Génie Electrique de Paris (LGEP) / SPEE-Labs, CNRS UMR 8507, SUPELEC,
Univ. Pierre Marie Curie (P6) et Univ. Paris Sud (P11), Plateau de Moulon
91192 Gif sur Yvette, France
olivier.bethoux@lgep.supelec.fr

Abstract- This paper is in the scope of fuel cell robust control. As a matter of fact, reliability and lifetime are the two major key points for fuel cell commercialization, especially as far as proton exchange membrane technology is concerned. To bring about these essential properties, the system designer needs to build a robust control law based on a suitable and on-line state of health knowledge. For this latter diagnosis purpose, we describe a new on-line impedance spectroscopy which gets accurate data while still allowing load monitoring.

I. INTRODUCTION

This article deals with a new approach to obtain in actual fuel cell system an on-line diagnosis in order to allow a robust control strategy for well monitoring operating cells conditions.

Fuel cell system is a complex and non-linear multi-physical and multi-scale system [1][2][3][4]. Moreover, fuel cell system seems to be vulnerable to operating conditions and, even if some degradation processes are not yet well understood, it seems important to operate close to the nominal conditions so as to slow down degradation [5][6][7]. For instance, water management of the PEM fuel cell is a key to reliable operation and slow degradation rate [8][9]. In that point of view, a good and continuous knowledge of the state of health of the fuel cell parts is essential for operating it in the right conditions. Many sensors (pressures, temperatures, voltages, current ...) are already set up and can be used for that purpose [10][11][12][13][14]. An accurate way of retrieving main fuel cells aspects (electro catalyst activity, membrane conductivity, mass transfer processes) is to obtain a wide range small signal frequency spectrum of its voltage and current [15]. This impedance spectroscopy technique is an expensive laboratory tool for off-line diagnosis [16]. The purpose of this article is to achieve on-line diagnosis based on this technique and hence to dramatically enhance the fuel cell state of health knowledge for relevant robust control.

This paper is organized in 6 sections. After this introduction, the second section briefly reviews fundamental concepts in fuel cells with particular emphasis on factors controlling their performance. Then, we detail the control design of the voltage regulator associated to the fuel cell. The fourth part deals with the best way to superimpose the monitored AC perturbation while regulating the load voltage. The fifth part is dedicated to achieve an accurate and noise insensitive AC retrieval. In this paragraph, we also compute

the parameters describing fuel cell state of health. In the last section, we draw the conclusions and perspectives of this work.

II. FUEL CELL BACKGROUND

Hydrogen fuel cell stacks facilitates the direct conversion of chemical energy to electricity and are made of N elementary cells electrically interconnected in series and fed in parallel with reactants [17]. Both reactants (H_2 and O_2 of the air) flow to the electrodes through diffusing layers. Oxidation reaction occurs in the anode and reduction reaction occurs in the cathode; electrode activity is enhanced by reactant concentration increase, electrode porosity rise and catalyst material. The stack voltage v_{FC} is a good characteristic of the stack efficiency; it can be written (1):

$$v_{FC} = N \cdot (E_{th} - v_{Ohm} - v_{act} - v_{mt}) \quad (1)$$

where:

- E_{th} is the theoretical cell voltage at zero current.
- $v_{Ohm} = R_m i_{FC}$ depicts the losses due to ionic current in the electrolyte, electronic current in the electrodes and contacts.
- $v_{act} = A_a \ln((i_{FC} + i_{L,loss})/i_0)$ is the Tafel law that describes the loss associated with overcoming the energy barrier to the electrode reaction.
- $v_{mt} = A_{mt} \ln(i_L/(i_L - i_{FC}))$ is closely linked to the Nernst law and takes the electrode concentration gradient into account (transport mechanism within the gas diffusion layer).

Proton Exchange Membrane (PEM) fuel cells fulfil compact systems requirements (portable power and road transportation) [18]. For this fuel cell type, the ionomer membrane protons conductivity depends strongly on the level of hydration in the membrane: low membrane water content results in a low ionic conductivity. Conversely, as the electrochemical reactions take place in the catalyst layer where gases, protons and electrons can participate, a high humidification rate results in a smaller three-phase boundary area due to local condensing: this phenomenon raises activation losses. Moreover, a flooded membrane electrode assembly induces partial or global reactants starvation: this phenomenon increases mass-transportation losses and even degrades the carbon electrode layer [5][6].

This small overview on fuel cell underlines that fuel cell efficiency and lifetime are closely related to its operating

conditions and that, in the case of PEM technology, water management is a key to reliable management and slow degradation processes. This robust control of the fuel cell first requires good information. The polarization curve is of great interest for understanding the state of health of the stack [19][20]. But this technique is only suitable for off-line analysis; cyclic voltamperometry has the same drawback [16]. But, even if fuel cell is a complex interplay of many non-linear phenomena and factors, each process (electrode reaction, gases diffusion, thermal transfer...) taking place in a fuel cell differs from time constants point of view. This leads to a ‘‘perturb and observe’’ approach known as impedance spectroscopy. This technique is commonly used in electrochemical devices and needs specific lab instruments [16]. It is based on a small AC signal disturbance which permits a linearized model fitting. It revealed to be relevant with fuel stack state of health observation and was successfully implement for laboratory PEMFC diagnosis purpose [15].

This article deals with the implementation of an accurate and non-disturbing continuous on-line impedance spectroscopy. This new system functionality will operate without bringing into play any further devices. One just modifies the control management law. A previous study already suggested the use of switching current ripples, but this method could only retrieve ohmic losses (membrane resistance) [21]. Another study proposed a wide frequency range scan but this technique switches between regulation goal and diagnosis monitoring [22]. The originality of this study is to offer a technique able to keep traditional tracking aspects while offering a wide range frequency analysis and hence a good and continuous state of health

To validate the whole approach (tracking, perturbing, useful signal retrieval and parameters fitting) we represent the fuel cell stack by a simple Randles circuit consisting of a couple of resistors and a capacitor (Fig. 1) [16]. The resistance (R_m) represents both electronic and ionic resistance, the capacitor (C) represents the double layer electrolyte – electrode parasitic capacitor, and finally the resistance (R_a) represents the charge transfer resistance (activation losses). The parameters we take into account for the whole study are listed in Table I. They are akin to the characteristics of the Nexa FC designed by Ballard.

TABLE I
FUEL CELL VALUES USED FOR SIMULATIONS

E_0	R_m	R_a	C
35 V	50 m Ω	250 m Ω	10 mF

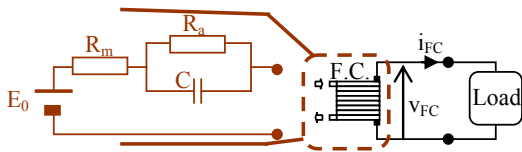


Fig. 1. Equivalent circuit representing the fuel cell

III. FUEL CELL SYSTEM AND ITS ASSOCIATED CONVERTER.

A. Output stage structure and its associated control

The previous section analyzed that power losses (activation, charge transfer and gas diffusion) involve a fuel cell voltage decrease as far as power demand increases. This voltage versus current dependency leads the integrator designer to add a voltage regulator between the stack electrical output and the application. As a matter of fact the voltage ratio between open circuit voltage (OCV) and nominal voltage (NV) often reaches $OCV / NV = 1.6$ in beginning-of-life conditions, and may rise up to 2 in end-of-life conditions. Loads rarely support such a voltage dynamic and usually need almost constant input voltage. As fuel cell stack is a low voltage – high current DC source, the required interface is often a set-up converter. The simplest way to implement this latter is to build a boost converter (Fig. 2), but several authors studied more optimized implementations [23].

The load voltage is the first objective of the regulator. The controller also aims to respect fuel cell constraints and especially to limit over-current. Unfortunately, the boost converter has a single control value: the PWM command. To overcome this challenge, we build imbricate control loops: high speed fuel cell current feedback driven by a low speed load voltage feedback. As a matter of fact, fuel cell current must be controlled very precisely whatever the operating conditions; this current needs a quick tracking in order to reject any perturbation. On the contrary, the fuel cell power can only change slowly due to the gases delivery response time, generally limited by the air blower. Transient specifications clearly depend on applications, but in case of rapid load changes (as it occurs in propulsion of cars), the general approach is to provide load pulse energy with appropriate power supply like ultra-capacitors [24][25]: so, in any case, the power demanded to the fuel cell and its associated boost converter has low frequencies content. This assessment justifies that the bus voltage control is a slow loop: hence, there is time decoupling between the fuel cell current requirement and bus voltage one.

B. The inner current loop

The boost inductance function is to convert the fuel cell voltage source into a current source; it is designed to obtain low current ripple at the switching frequency. So, in a control purpose, the inductance impedance is the dominating term compared to fuel cell internal impedance. In that sense, the

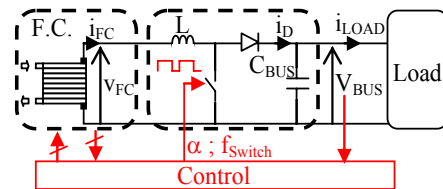


Fig. 2. schematic diagram of an integrated fuel cell system.

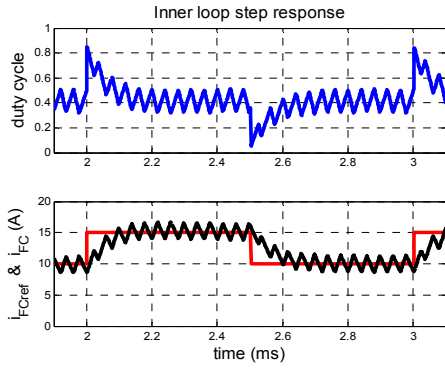


Fig. 3. Inner loop step response (DC chopper operating at $F_{\text{Switch}} = 25$ kHz).

fuel cell and boost interaction is described with the following equation (2):

$$L \cdot di_{FC}/dt = v_{FC} - (1-d)V_{BUS} \quad (2)$$

with d , the duty cycle of the PWM command, being the effective control variable. The inductance value is: $L = 200 \mu\text{H}$

As $v_{FC}(t)$ voltage is sensed for a diagnosis purpose, the control strategy can use it for compensation. $V_{BUS}(t)$ is a slow variable and can be considered constant during $i_{FC}(t)$ tracking which makes the link between the control variable (d) and the measured variable ($i_{FC}(t)$) a linear equation. Assuming (3)

$$\beta = -(1 - d - (v_{FC}/V_{BUS})) \quad (3)$$

the open loop transfer function is:

$$i_{FC}(s)/\beta(s) = V_{BUS} / (Ls) \quad (4)$$

Hence, we can design a classical PI regulator ($K_P = 0.05$; $K_I = 160$). Fig. 3 depicts a step response of this fast inner current loop. Its dynamics is tuned in order to get a time response of about 5 switching periods.

C. The outer voltage loop

At that point, we now need to build the fuel cell current reference value with the second cascaded loop in order to monitor the bus voltage. Considering no chopper losses and that the inductor L is a small storage device compared to C_{BUS} capacitor, one computes the following set of equation:

$$C_{BUS} dV_{BUS}/dt = i_D - i_{LOAD} \quad (5)$$

$$v_{FC} i_{FC} = V_{BUS} i_D \quad (6)$$

Both $V_{BUS}(t)$ and $V_{FC}(t)$ are measured, so we can linearize this equation by substituting the new variable (i_D) for the actual control variable (i_{FC}). Hence (5) becomes a first order linear equation where (i_D) is the virtual control value and $i_{LOAD}(t)$ acts as a slow perturbation. To respect dynamics decoupling as well as fuel cell air supply constraints, this second control loop is tuned so that the ratio between outer and inner time responses is larger than 20. This second regulator is also a PI corrector.

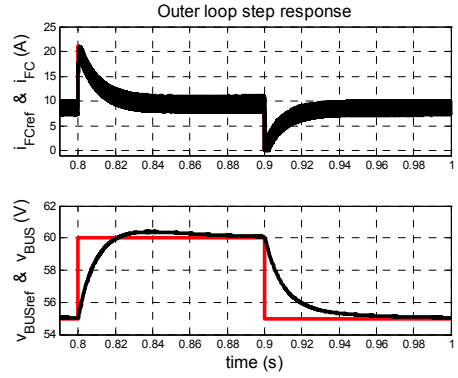


Fig. 4. Outer loop step response : $i_{FC}(t)$ and $v_{BUS}(t)$

Fig. 4 represents a step response (rising and falling hedges) of this outer voltage loop even if it normally operates in regulation mode rather than tracking mode. The controller parameters are chosen to obtain a dominating pole with a 10 Hz cut-off frequency ($K_P = 2.5$; $K_I = 60$).

IV. PERTURBATION INSERTING

A. General description

The previous section explained that the fuel cell is always connected to its electrical load with a voltage regulator. This latter has two objectives: it must maintain the load reference voltage whatever the power demand, and it must guarantee that the fuel cell electrical variables (v_{FC} and i_{FC}) always match the fuel cell requirements whatever the operating conditions are. As impedance spectroscopy revealed itself a very relevant non-invasive diagnosis technique for evaluating fuel cell state of health [15], we intend to use the power interface and its sensors to embed this new functionality. For that purpose, we both need to keep the previous control system and to add a small and well-known sinusoidal fuel cell current over a wide range of frequencies (roughly from less than 1 Hz to 1 kHz or greater). Our idea is to keep the global control structure and only to find the best way to introduce the perturbation signal.

B. AC Current insertion

As we internally monitor the fuel cell current, the first idea is to add the desired AC perturbation to the current reference value computed by the outer loop (Fig. 5). This solution is effective (Fig. 6) as far as the imposed frequency remains far out of the outer loop bandwidth. In this case (Fig. 6), the added signal is almost not compensated. In this example, the desired AC current characteristics are 1 A and 100 Hz. This AC current is actually achieved (second scope) and induces an AC bus voltage swing (third scope). This swing is measured and is fed back to the outer loop. As this signal is out of the voltage corrector bandwidth, the controller is unable to modify the current reference (first scope). Otherwise, at low frequency (Fig. 7), the actual current reference (i_{FC_ref}) no longer contains the expected AC amplitude. As a matter of fact, when superimposing an AC current (i_{FC_pert}) to the regulator required current (i_{FC_regV}), one induces an alternative power which flows from the fuel cell to

the DC bus through the switching converter. This means that the bus voltage also fluctuates. This fluctuation is measured and the voltage controller aims to cancel it by building the appropriate fuel cell current. In Fig. 7, the demanded AC current characteristics are (1 A ; 5 Hz) and the result is no longer achieved (second scope). The controller output signal merely compensates the injected AC signal making the strategy ineffective (first scope).

C. AC Voltage insertion

For low frequencies (in the voltage bandwidth range), the idea is to superimpose a small AC voltage $v_{BUS_pert}(t)$ to the bus reference value V_{REF} (Fig. 8). In this way, one also induces an alternative power responsible for fuel cell voltage and current ripples: hence, the desired effect is achieved. The

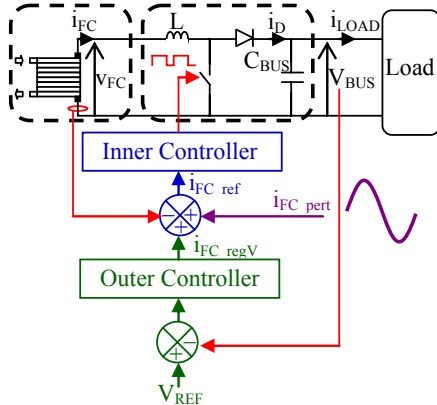


Fig. 5. AC perturbation by superposing an AC current

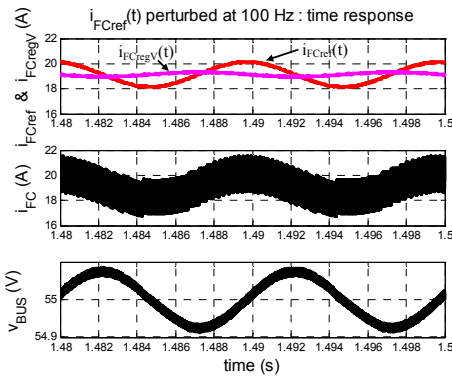


Fig. 6. AC perturbation superimposed to the voltage controller output (100 Hz)

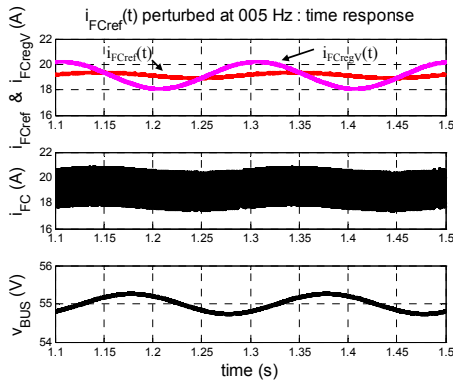


Fig. 7. AC perturbation superimposed to the voltage controller output (5 Hz)

only concern is to forecast the amplitude of the fuel cell signals so as to be sure that the linearity assumption remains valid which is a key criterion for good impedance measurements. For that purpose, we evaluate the AC swing in the worse case. Neglecting the energy stored in the inductance (low frequency case) and assuming no losses in the DC converter, power balance equation is:

$$V_{BUS} C_{BUS} d(V_{REF} + v_{BUS_pert})/dt = (V_{FC} + v_{FC_pert})(I_{FC} + i_{FC_pert}) \quad (8)$$

Hence, for small perturbation signals, we can evaluate the AC fuel cell current i_{ref_pert} :

$$i_{ref_pert} = \frac{j\omega_{pert} C_{BUS} V_{BUS} v_{BUS_pert}}{V_{FC} + Z_{FC} I_{FC}} \quad (9)$$

The fuel cell impedance is somehow unknown but, at any frequency, we have a good idea of its boundaries; this allows us to forecast roughly the AC current amplitude which is sufficient for aiming small perturbation criterion. But, in a future work, we will study, the possibility of keeping constant this amplitude in order to respect linearity requirement.

Fig. 9 illustrates the approach dedicated to low frequency AC signals (5 Hz). For the test, the AC bus voltage amplitude is computed with (9) and the assumption that $Z_{FC} \cong R_m + R_a$.

D. Final control architecture scheme

Fig. 10 gives an overview of our perturbation implementation. Depending on the frequency range, one

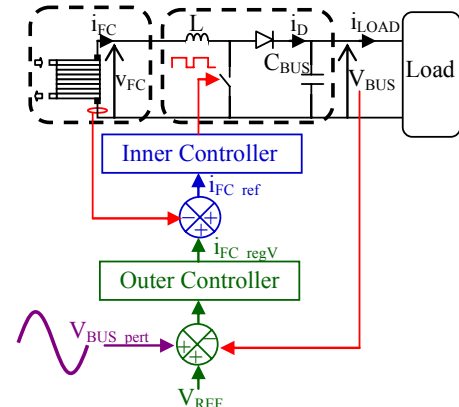


Fig. 8. AC perturbation by superposing an AC voltage

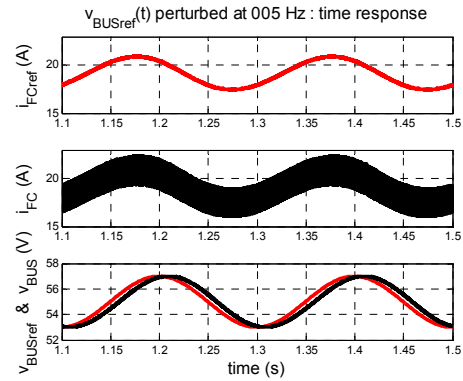


Fig. 9. AC perturbation superimposed to the constant reference of the voltage controller (5 Hz)

switches the perturbation signal either to the inner loop reference value ($f_{\text{pert}} > f_{\text{select}}$) or to the outer loop reference value ($f_{\text{pert}} < f_{\text{select}}$). The frequency (f_{select}) is designed so as to be sure that the outer loop is unable to compensate the AC superimposed current (which practically means a -20 dB attenuation ratio).

To conclude this part, we point out that this strategy allows regulating the load voltage without any delay, even when operating a spectroscopy measurement. Hence, the first functionality of the electrical power interface device is guaranteed. Fig. 11 illustrates such tracking reaction under measuring process. Note that $v_{\text{BUS}}(t)$ remains very close to its reference value ($V_{\text{REF}} = 55 \text{ V}$) due to the voltage control. Without regulation, such a disturbing load ($\Delta I_{\text{LOAD}} = 2 \text{ A}$; $f_{\text{LOAD}} = 2 \text{ Hz}$) would have produced huge AC bus voltage ripples: roughly 16V amplitude.

V. USEFUL SIGNAL MONITORING AND PARAMETERS IDENTIFICATION

The previous section explained how to impose a small sinusoidal current of known amplitude and frequency to the fuel cell stack while still operating the regulation process. This part is dedicated to argue how to monitor the small AC perturbation. Our main argument is that we know very precisely the monitored frequency as we impose it. This fact allows to implement synchronous detection. By multiplying each variable (i_{FC} and v_{FC}) with the imposed frequency, the useful signal is always translated to a null frequency.

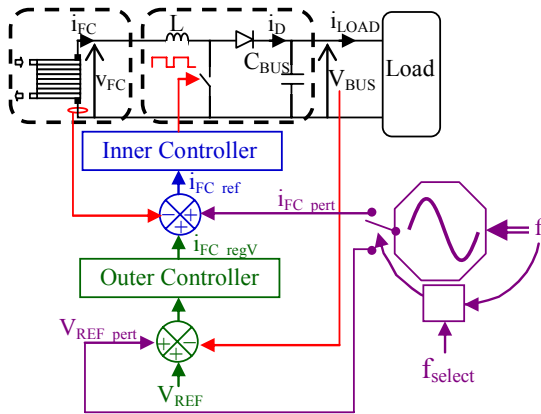


Fig. 10. strategy for superposing an AC perturbation

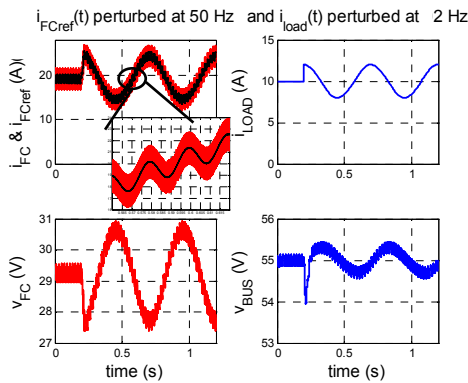


Fig. 11. AC perturbation superimposed to the voltage controller output (50 Hz) while a AC perturbation occurs at the load side (2 Hz)

Assuming a constant load, fuel cell current can be written as:

$$i_{\text{FC}}(t) = I_{\text{FC}} + I_{\text{FC_pert}} \cos(\omega t + \phi_1) \quad (10)$$

By multiplying (10) by $\cos(\omega t)$, one gets (11):

$$i_{\text{FC}}(t) \cos(\omega t) = (I_{\text{FC_pert}}/2 \cos(\phi_1)) + (I_{\text{FC}} \cos(\omega t)) + (I_{\text{FC_pert}}/2 \cos(2\omega t + \phi_1)) \quad (11)$$

It becomes easy to obtain the useful signal: a low pass filter retrieves the useful continuous component and rejects the undesired components ranging at ω and 2ω . Thus, the set of filter design specification is described as follows:

- The stopband corner frequency is the monitored frequency ω .
- The low pass filter has at least 52 dB stopband attenuation so as to insure a $(I_{\text{FC_pert}}/(2I_{\text{FC}}))$ ratio lower than 1/10.
- The time response has to be as small as possible to allow fast processing.

This filter specification design leads to a digital fourth order transfer function, which will be easy to implement with microprocessor devices. The 1% step response of this filter corresponds to 372 samples; so the measurement of I_X and V_X components will occur after 500 samples which means after 25 perturbation signal periods. The measurement sequence lasts 2 periods which enables us to make an average calculation which cancels the undesired signal part.

As the final aim is to compute the complex impedance $Z(\omega)$, we need to get both amplitude and phase of each electrical variables $i_{\text{FC}}(\omega)$ and $v_{\text{FC}}(\omega)$. For that purpose, it is easier to obtain the useful signal in a Fresnel framework. For that reason, both signals are multiplied with $\cos(\omega t)$ and

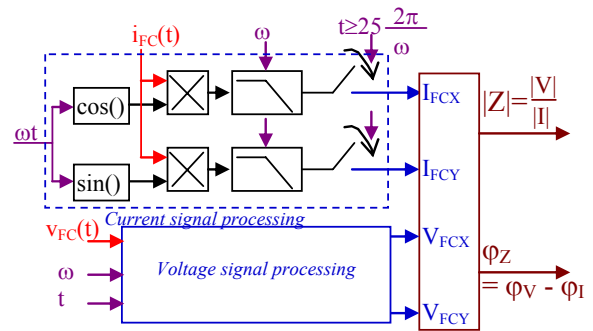


Fig. 12. Monitoring strategy scheme

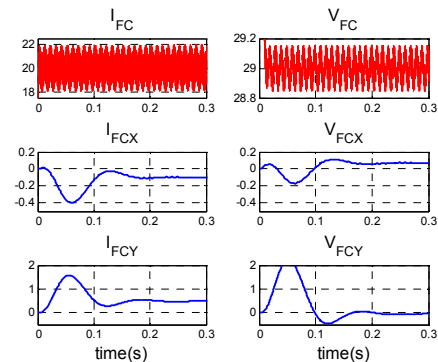


Fig. 13. Monitoring time response (AC perturbation at 100 Hz)

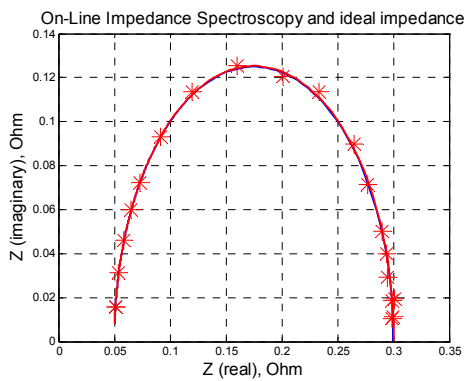


Fig. 14. Nyquist diagram (stars based on monitoring, line based on Randles structure)

$\sin(\omega t)$ which makes us able to get the real components (I_X and V_X) as well as the imaginary components (I_Y and V_Y). Fig. 12 represents the monitoring strategy, while Fig. 13 gives an example with 100 Hz AC perturbation. This strategy reveals effective and we get accurate Nyquist points over the [1 Hz ; 1 kHz] range as shown on the Nyquist diagram (Fig. 14). Those 20 frequency response data allow computing the Randle structure parameters with a least squares method.

VI. CONCLUSION AND PERSPECTIVES

This article is within the scope of fuel cell robust control. For this purpose, the controller needs to know precisely the fuel cell operating conditions. In order to obtain the fuel cell parameters, an on-line spectroscopy method is described. The presented strategy achieves to retrieve the small signal fuel cell model without any electrical load disturbances. This novel method is able to scan the wide range of frequencies needed for a fuel cell characterization. It does not require any further devices since it uses the DC-DC converter and its associated controllers. In this paper, the small AC perturbation signal injection is detailed. Moreover, the signal processing method is explained; it extracts the useful components in order to compute the Randles circuit parameters by force-fitting to simulated data.

The perspective of this work is to experiment our technique on the LGEP fuel cell test bench. The main concerns will be: to determine how complex the fuel cell model structure should be to describe the major physical phenomenon, to adjust the scanned frequencies number, to consider the importance of monitoring each single cell voltage rather than solely the whole stack voltage.

REFERENCES

- [1] K. Haraldsson and K. Wipke, "Evaluating fuel cell system models", *Journal of Power Sources*, vol.126, n°1-2, 2004, pp. 88-97.
- [2] F. Gao, B. Blunier, A. Miraoui, and A. El Moudni, "A multiphysic dynamic 1D model of a proton exchange membrane fuel cell stack for real time simulation", *Industrial Electronics, IEEE Transactions on Industrial Application*, in press, 2009.
- [3] B. Blunier and A. Miraoui, "Modelling of fuel cells using multi-domain VHDL-AMS language", *Journal of Power Sources*, 177 (2008), pp. 434-450
- [4] P.J.H. Wingelaar, J.L.Duarte, and M.A.M. Hendrix, "Dynamic Characteristics of PEM Fuel Cells", *IEEE 36th Power Electronics Specialists Conference, PESC '05, Recife, 2005*
- [5] S.D. Knights, K. M. Colbow, J. St-Pierre, and D.P. Wilkinson, "Aging mechanisms and lifetime of PEFC and DMFC", *Journal of Power Sources*, vol.127, 2004, pp. 127-134.
- [6] A. Taniguchi, T. Akita, K. Yasuda and Y. Miyazaki, "Analysis of electrocatalyst degradation in PEMFC caused by cell reversal during fuel starvation", *Journal of Power Sources*, vol.130, 2004, pp. 42-49.
- [7] N. Wagner and E. Gülzow, "Change of electrochemical impedance spectra (EIS) with time during CO-poisoning of the PT-anode in a membrane fuel cell", *Journal of Power Sources*, vol.127, 2004, pp. 341-347.
- [8] J.-M. Le Canut, R. Latham, W. Mérida, and D. A. Harrington, "Impedance study of membrane dehydration and compression in proton exchange membrane fuel cells", *Journal of Power Sources*, 2009, in press.
- [9] A.Y. Karnik, J.H. Bukland, and J. Sun, "Performance of a PEM fuel cell water management system using static output feedback" *IEEE American Control Conference, USA New-York Cit, 2007*.
- [10] D. Hissel, M.C. Péra, J.M. Kauffmann, "Diagnosis of automotive fuel cell power generators", *Journal of Power Sources*, vol. 128, 2004, pp. 239-246
- [11] Ari Ingimundarson, Anna G. Stefanopoulou, and Denise A. McKay,, "Model-Based Detection of Hydrogen Leaks in a Fuel Cell Stack", *IEEE Transactions on Control Systems Technology*, Vol. 16, N° 6, September 2008.
- [12] L. A. M. Riascos, M. G. Simoes, P. E. Miyagi, "A Bayesian network fault diagnostic system for proton exchange membrane fuel cells", *Journal of Power Sources*, vol. 165, 2007, pp. 267-278
- [13] G. Tian et al., "Diagnosis methods dedicated to the localisation of failed cells within PEMFC stacks", *Journal of Power Sources*, vol. 182, 2008, pp. 449-461.
- [14] T. Escobet, D. Feroldi, S. de Lira, V. Puig, J. Quevedo, J. Riera, M. Serra, "Model based fault diagnosis in PEM fuel cell systems", *Journal of Power Sources (2009) in press*
- [15] N. Fouquet, C. Doulet, C. Nouillant, G. Dauphin-Tanguy, B. Ould-Bouamama, "Model based PEM fuel cell state-of-health monitoring via ac impedance measurements", *Journal of Power Sources*, vol. 159, 2006, pp. 905-913.
- [16] M. E. Orazem, and B. Tribollet, *Electrochemical Impedance Spectroscopy*. Wiley Interscience, sept. 2008.
- [17] F. Barbir, *PEM Fuel Cells: Theory and Practice*. Elsevier Academic Press, New-York, june 2005.
- [18] P. Zegers, "Fuel cell commercialization: The key to a hydrogen economy", *Journal of Power Sources*, vol. 154, 2006, pp. 497-502.
- [19] G. Fontes, C. Turpin, and S. Astier, "A large signal dynamic circuit model of a H2/O2 PEM fuel cell: description, parameter identification and exploitation", *Fundamentals and Developments of Fuel Cells Conference, FDFC'2008, France Nancy, dec. 2008*.
- [20] Williams, Kunz and Fenton, "Analysis of polarization curves to evaluate polarization sources in hydrogen/air PEM fuel cells," *Journal of the Electrochemical Society*,152, A635-A644, 2005.
- [21] M. Hinaje, I. Sadli, P. Thounthong, J.-P. Martin, S. Raël, and B. Davat, "An additional use of the boost converter as a diagnosis device of the PEMFC humidification", *FDFC'2008, France Nancy, dec. 2008*
- [22] A. Narjiss, D. Depernet, D. Caqundusso, F. Gustin, and D. Hissel, "On-line diagnosis of a PEM fuel cell through the PWM converter", *FDFC'2008, France Nancy, dec. 2008*
- [23] Alexandre De Bernardinis, et al, "Fuel cells multi-stack power architectures and experimental validation of 1 kW parallel twin stack PEFC generator based on high frequency magnetic coupling dedicated to on board power unit", *Energy Conversion and Management*, vol 49, 2008, pp. 2367-2383.
- [24] P. Thounthong, S. Raël, and B. Davat, "Control Strategy of Fuel Cell and Supercapacitors Association for a Distributed Generation System" *IEEE Transactions on Industrial Electronics*, vol. 54, n° 6, December 2007.
- [25] T. Azib, O. Bethoux, G. Remy and C. Marchand, "Structure and Control Strategy for a Parallel Hybrid Fuel Cell/Supercapacitors Power Source" *IEEE VPPC'09 in Dearborn, Michigan, USA, September 7-11, 2009*.